Influence of Minor Groove Substituents on the Structure of DNA Holliday Junctions†

Franklin A. Hays, Zebulon J. R. Jones, and P. Shing Ho*

Department of Biochemistry and Biophysics, ALS 2011, Oregon State University, Corvallis, Oregon 97331

Received March 18, 2004; Revised Manuscript Received May 26, 2004

ABSTRACT: The inosine-containing sequence d(CCIGT*ACm*^{5}*C*GG) is shown to crystallize as a four-stranded DNA junction. This structure is nearly identical to the antiparallel junction formed by the parent d(CCGGT*ACm*^{5}*C*GG) sequence [Vargason, J. M., and Ho, P. S. (2002) *J. Biol. Chem. 277*, 21041−21049] in terms of its conformational geometry, and inter- and intramolecular interactions within the DNA and between the DNA and solvent, even though the 2-amino group in the minor groove of the important G_3•m^5C_8 base pair of the junction core trinucleotide (italicized) has been removed. In contrast, the analogous 2,6-diaminopurine sequence d(CCDGTACTGG) crystallizes as resolved duplex DNAs, just like its parent sequence d(CCAGTACTGG) [Hays, F. A., Vargason, J. M., and Ho, P. S. (2003) *Biochemistry 42,* 9586−9597]. These results demonstrate that it is not the presence or absence of the 2-amino group in the minor groove of the R_3•Y_8 base pair that specifies whether a sequence forms a junction, but the positions of the extracyclic amino and keto groups in the major groove. Finally, the study shows that the arms of the junction can accommodate perturbations to the B-DNA conformation of the stacked duplex arms associated with the loss of the 2-amino substituent, and that two hydrogen bonding interactions from the C_7 and Y_8 pyrimidine nucleotides to phosphate oxygens of the junction crossover specify the geometry of the Holliday junction.

DNA Holliday junctions are ephemeral intermediates that have been implicated in the mechanisms of a large number of biological processes. A four-stranded DNA junction was proposed by Holliday more than 40 years ago (*1*) to help explain the process of gene conversion in yeast and has since been implicated in a diverse array of related mechanisms, including genetic recombination, DNA repair, and viral integration (*2*−*6*). The involvement of these structural intermediates over such a broad range of biological processes, typically serving to protect and expand the coding potential of genomes, has made junctions the focus of intense study. A recent series of single-crystal structures reveal how interactions between the major groove of the double-helical arms and the phosphates at the junction crossover help to define the formation of these complexes. We present here a systematic study to elucidate the contribution of the minor groove 2-amino substituent groups to the formation of four-stranded junctions in crystals.

The conformation of DNA Holliday junctions is now understood to be highly variable. Solution studies have shown that junctions exist in two general conformations: the open-X and stacked-X forms (Figure 1). The open-X form predominates under low-salt conditions, with the four B-DNA arms arranged in essentially a square planar configuration to minimize the electrostatic interactions between the negatively charged phosphates of the phosphoribose backbones. High concentrations of monovalent and divalent cations help to shield these phosphates, allowing the junction to assume the more compact stacked-X structure in which the arms are coaxially stacked to form two semicontinuous B-DNA duplexes. In the stacked-X structure, the strands of the B-DNA arms can, in theory, assume either a parallel or antiparallel relationship (*7*, *8*). To date, only the antiparallel form has been definitively observed in solution (*8*, *9*). Furthermore, the duplexes of the antiparallel stacked-X junction can be related in a left- or right-handed orientation (Figure 1c). The antiparallel junction can be locked in one specific isomeric form or can be dynamic and readily switch between forms with the open-X structure serving as an intermediate (*10*−*12*).

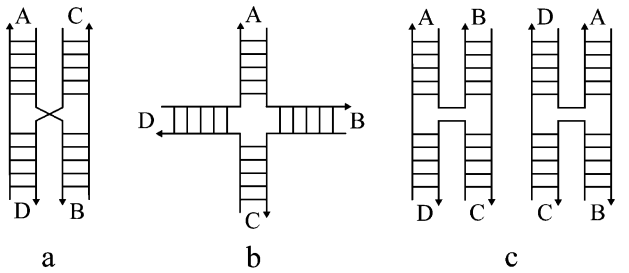

FIGURE 1: Three general forms of DNA Holliday junctions: (a) parallel stacked-X, (b) open-X, and (c) antiparallel stacked-X. The stacked-X form is generated by the coaxial stacking of B-DNA arms of the open-X form onto one another to form pseudocontinuous B-DNA duplexes.

† This work was supported by grants from the National Institutes of Health (R1GM62957A) and the National Science Foundation (MCB-0090615). The X-ray diffraction facilities are supported by the Proteins and Nucleic Acids Facility Core of the Environmental Health Sciences Center at Oregon State University (NIEHS ES00210) and a grant from the Murdock Charitable Trust. Access to BioCARS Sector 14 was supported by the National Institutes of Health, National Center for Research Resources, under Grant RR07707.

* To whom correspondence should be addressed. Phone: (541) 737-2769. Fax: (541) 737-0481. E-mail: hops@onid.orst.edu.

10.1021/bi049461d CCC: $27.50
Published on Web 07/10/2004

Several single-crystal structures of these important biological intermediates have now been determined at the atomic level (reviewed in refs *13* and *14*). Comparison of junction-forming sequences has identified a trinucleotide core motif as being key to the formation of these four-stranded structures. The sequence of this trinucleotide core was originally defined as $A_6C_7C_8$ (*15*), but later expanded to $Pu_6C_7Py_8$, where Pu[1] is either the adenosine or guanosine purine nucleotide and Py can be a cytosine, 5-methylcytosine (m^5C), or 5-bromouridine (br^5U) pyrimidine-type nucleotide, but not thymidine (*16*). These nucleotides are involved in a number of crucial interactions that link the major groove surfaces of the stacked duplex arms to the crossover phosphates. Atomic force microscopy (AFM) and nuclease digestion studies on synthetic junctions that incorporate the core ACC trinucleotide show the same overall geometry and crossover topology that are exhibited by the crystal structures (*17*).

The conformation of junctions in solution and in the crystals appears to be related to these sequence-dependent intramolecular interactions. A detailed comparison of the available crystal structures shows that the junctions can be grouped into two classes. Those structures that show a set of direct hydrogen bonding interactions, between (i) the Py_8 base and the O2P phosphate oxygen of C_7, (ii) the outside G_3 nucleotide and the O1P phosphate oxygen of Pu_6, and (iii) the N4 amino group of C_7 and the O1P phosphate oxygen of Pu_6, have a well-defined geometry, while structures in which one or more of these interactions are missing or mediated by solvent show greater variability in conformation (*13*). Thus, it has become increasingly clear that the nucleotides within, and adjacent to, the crossover region of DNA Holliday junctions play key roles in defining the global geometry and formation of the stacked-X conformation.

Up to this point, it has not been clear what effect interactions in the minor groove may have on the formation and geometry of the junction. For example, a hexaaquocalcium(II) ion has been observed in the minor groove as a common feature of the junction arms in several of the higher-resolution structures, which may play an electrostatic role in stabilizing the complex. The currently available structures, however, do not directly tell us how important the substituent interactions are in this narrow groove. The sequence d(CCGGTACm^{5}CGG) forms a junction (*18*), but d(CCAGTACTGG) does not (*16*). In this comparison, we see that the extracyclic amino and keto substituents at the major groove surface are switched between the G_3·m^5C_8 and A_3·T_6 base pairs, but the difference in conformation may arise instead from the lack of a 2-amino group in the minor groove of the A_3·T_6 base pairs of the latter sequence. To distinguish between the effects of minor groove and major groove substituents, we have studied the single-crystal structures of the sequences d(CCIGTACm^{5}CGG), in which the G_3 nucleotide of d(CCGGTACm^{5}CGG) is replaced with an inosine (I) which thus removes the amino group from the minor groove, and the sequence d(CCDGTACTGG), in which an amino group is added to the A_3 nucleotide of d(CCAGTACTGG) to introduce a 2,6-diaminopurine (D) at this position.

[1] Abbreviations: Pu, purine; Py, pyrimidine; I, inosine; D, 2,6-diaminopurine; AFM, atomic force microscopy; SD, standard deviation.

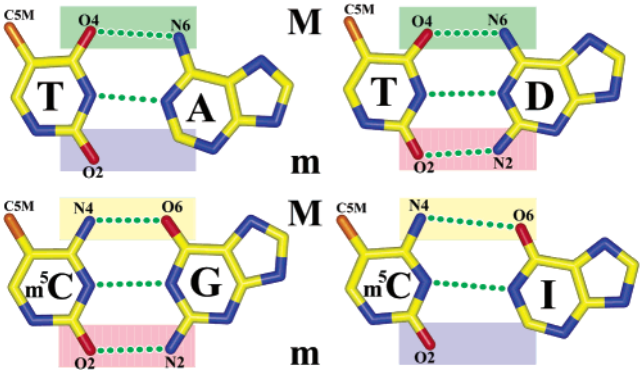

FIGURE 2: Standard and modified nucleotide base pairs located in the R_3-Y_8 base pair step. Exocyclic substituents are labeled with the location of the major (M) and minor (m) groove faces denoted adjacent to each base pair. An I·m^5C base pair is similar to a G·m^5C base pair from the major groove face (light yellow) and an A·T base pair from the minor groove face (light blue). A D·T base pair is similar to an A·T base pair from the major groove (light green) and a G·m^5C base pair from the minor groove (light red). All base pairs have standard Watson−Crick hydrogen bonding interactions as indicated by green circles between each base. 5-Methylcytosine bases are used for consistency with the parent d(CCGGTACm^{5}CGG) junction structure and thymidine nucleotides in the Y_8 position.

The modified bases inosine and 2,6-diaminopurine have long been used to study the effect of minor groove interactions on DNA conformation, showing how the 2-amino group affects the flexibility (*19*, *20*), minor groove width and solvent interactions (*21*−*23*), endonuclease cleavage (*24*, *25*), and molecular recognition (*26*−*28*) of the DNA duplex. In the current study, I and D nucleotides are placed in key positions of the conserved trinucleotide core sequence, where we have identified important junction-stabilizing interactions. The D_3·T_8 base pairs in the d(CCDGTACTGG) sequence are A·T-like in the major groove and G·C-like in the minor groove. Conversely, the I_3·m^5C_8 base pairs of d(CCIGTACm^5-CGG) are G·C-like in the major groove and A·T-like in the minor groove, both with standard Watson−Crick hydrogen bonding interactions and methyl groups at C5 of the pyrimidine base (Figure 2). We observe that d(CCDGTACTGG) crystallized as resolved B-DNA duplexes while d(CCIGTACm^{5}CGG) formed a DNA Holliday junction, thus further supporting the model that it is the interactions between the major groove and crossover phosphates that determine junction formation in the crystal system (*13*, *15*, *16*, *18*). Additionally, we see that minor groove interactions do not significantly contribute to the global geometry of the resulting junction structure.

MATERIALS AND METHODS

All deoxyoligonucleotides were synthesized using solid phase phosphoramidite chemistry with the trityl-protecting group left attached to the 5′-terminal hydroxyl group to facilitate subsequent purification from failure sequences via reverse phase HPLC. Preparative reverse phase HPLC was performed using a Microsorb 300 Å pore size C-18 column measuring 250 mm × 21.4 mm (inside diameter) at a flow rate of 8 mL/min in 0.1 mM triethylamine acetate with an acetonitrile gradient. The full-length sequence typically eluted ~31 min postinjection in a mobile phase concentration of 20% acetonitrile. Purified tritylated DNA was deprotected

by treatment with 3% aqueous acetic acid for 15 min with gentle agitation, neutralized with concentrated ammonium hydroxide, and desalted on a Sigma G-25 Sephadex column, yielding purified DNA. Purified DNA was stored at −80 °C as a lyophilized powder and resuspended in deionized double-distilled water prior to use. All crystals were grown in 10 μL sitting drops by the vapor diffusion method and equilibrated against a 30 mL reservoir volume.

Crystallization and Structure Solution of d(CCIGTACm^{5}CGG). Thin diamond crystals of d(CCIGTACm^{5}CGG) (monoclinic *C*2 space group; dimensions $a = 64.92$ Å, $b = 24.87$ Å, $c = 37.10$ Å, and $\beta = 109.22°$) were grown from solutions containing 25 mM sodium cacodylate (pH 7.0), 0.5 mM DNA, 180 mM $CaCl_2$, and 2.4 mM spermine tetrahydrochloride equilibrated against 20% (v/v) 2-methyl-2,4-pentanediol (MPD) at 25 °C. X-ray diffraction data to 2.0 Å resolution were collected at liquid nitrogen temperatures using Cu Kα radiation from a Rigaku (Tokyo) RU-H3R rotating anode generator operating at 50 kV and 100 mA with an Raxis-IV image plate detector on a single crystal measuring 0.55 mm × 0.25 mm × 0.05 mm. An artificial mother liquor containing 25% MPD was used for cryoprotection. The space group and unit cell dimensions of d(CCIGTACm^{5}CGG) are very similar to those of previous junction crystals of the parent d(CCGGTACm^{5}CGG) sequence, with two strands in the asymmetric unit (asu). Thus, a search model using the d(CCGGTACm^{5}CGG) junction (*18*) was used in EPMR (*29*) to determine the structure by molecular replacement, initially to 3.0 Å resolution. A distinct solution with a correlation coefficient of 77.5% and an R_{cryst} of 36.23% was obtained with two unique strands in the asu adjacent to a crystallographic 2-fold symmetry axis. A simulated annealing omit map with the C_7 crossover phosphate removed showed distinct $F_o - F_c$ density within the crossover region indicative of a DNA Holliday junction. Subsequent refinement of this initial junction structure in CNS (*30*) using rigid body refinement, simulated annealing, several rounds of positional and individual *B*-factor refinement, and addition of solvent resulted in a final R_{cryst} of 23.57% and an R_{free} of 25.82% (Table 1).

Crystallization and Structure Solution of d(CCDGTACTGG). Long rodlike crystals of d(CCDGTACTGG) were grown at room temperature in 5 mM Tris-HCl (pH 7.5), 23 mM calcium acetate, 0.6 mM DNA, and 16% MPD equilibrated against a reservoir solution of 28% MPD. Crystals were flash-frozen directly out of the drop prior to data collection. Data for a crystal measuring 0.30 mm × 0.1 mm × 0.1 mm in size were collected to 1.85 Å resolution at liquid nitrogen temperatures on BioCARS beamline 14-BMC at the Advanced Photon Source (Argonne National Laboratory, Argonne, IL) with 0.9 Å radiation. The crystals were indexed in hexagonal space group $P6_122$, are isomorphous to the crystals of the parent d(CCAGTACTGG) sequence, and have the following unit cell dimensions: $a = 32.96$ Å, $b = 32.96$ Å, and $c = 88.56$ Å. The structure of d(CCDGTACTGG) was determined by molecular replacement using the coordinates of the d(CCAGTACTGG) structure (UD0030). An EPMR search (against 3.0 Å data) using this initial search model of one strand adjacent to a crystallographic symmetry axis produced a correlation coefficient of 77.1% and an R_{cryst} of 37.5%. The initial round of rigid body and rigid parts refinement on this model followed by simulated annealing produced a starting R_{cryst} of 35.31% and an R_{free} of 38.80%. Structure refinement was carried out in CNS using standard positional and individual *B*-factor refinement followed by assignment of solvent molecules, producing a final R_{cryst} of 23.21% and an R_{free} of 25.83% (Table 1).

Table 1: Data Collection and Refinement Statistics

	d(CCIGTACm^{5}CGG)	d(CCDGTACTGG)
	Data	
unit cell		
a (Å)	64.92	32.96
b (Å)	24.87	32.96
c (Å)	37.10	88.56
β (deg)	109.22	-
space group	*C*2	$P6_122$
total no. of reflections	9439	34659
no. of unique reflections	3492	2528
resolution (Å)	18.2−2.0	17.5−1.85
completeness (%)[a]	93.4 (61.8)	96.3 (72.2)
$I/\sigma(I)$[a]	15.8 (2.4)	29.9 (4.98)
R_{merge} (%)[a,b]	5.0 (29.1)	5.6 (24.5)
	Refinement	
resolution (Å)	18.2−2.2	17.5−1.90
R_{cryst} (R_{free}) (%)[c]	23.57 (25.82)	23.21 (25.83)
no. of DNA atoms	404	203
no. of solvent atoms	62	45
average *B*-factor (Å^2) for DNA atoms (solvent atoms)	11.1 (11.7)	10.9 (20.6)
rmsd for bond lengths (Å)[d]	0.003	0.067
rmsd for bond angles (deg)[d]	0.8	6.2
structural conformation	Holliday junction	B-DNA

[a] Values in parentheses refer to the highest-resolution shell. [b] $R_{merge} = \sum_{hkl}\sum_i|I_{hkl,i} - \langle I\rangle_{hkl}|/\sum_{hkl}\sum_i|I_{hkl,i}|$, where I_{hkl} is the intensity of a reflection and $\langle I\rangle_{hkl}$ is the average of all observations of this reflection and its symmetry equivalents. [c] $R_{cryst} = \sum_{hkl}|F_{obs} - kF_{calc}|/\sum_{hkl}|F_{obs}|$. $R_{free} = R_{cryst}$ for 10% of the reflections that were not used in refinement (*51*). [d] Root-mean-square deviation of bond lengths and angles from ideal values.

All data were processed and reflections merged and scaled using DENZO and SCALEPACK from the HKL suite of programs (*31*). Resolution cutoffs were determined according to $\langle I/\sigma(I)\rangle$, completeness, R_{merge}, and R_{meas} statistics. R_{meas} was determined using the program available at http://loop8.biologie.uni-konstanz.de/~kay/, and root-mean-square deviation (rmsd) values were calculated using the McLachlan algorithm as implemented in ProFit version 2.2 (http://www.bioinf.org.uk/software/profit/) (*32*). Structural analysis was performed using CURVES 5.2 (*33*). The coordinates and structure factors have been deposited in the Protein Data Bank (*34*) as entries 1S1L for d(CCIGTACm^{5}CGG) and 1S1K for d(CCDGTACTGG).

RESULTS

Major and minor groove interactions are known to affect the local and global conformation of nucleic acid structures (*35*−*38*). The crystal structures presented here elucidate the role of nucleotide substituent groups in the minor groove and, by extension, the major groove in the formation of DNA Holliday junctions. The sequence d(CCIGTACm^{5}CGG) was seen to crystallize as a DNA Holliday junction, while d(CCDGTACTGG) crystallized as resolved B-DNA duplexes. In terms of base substituents, D·T base pairs from the major groove are A·T-like and from the minor groove are G·C-like while I·m^{5}C base pairs from the major groove are G·C-like and from the minor groove are A·T-like. Thus,

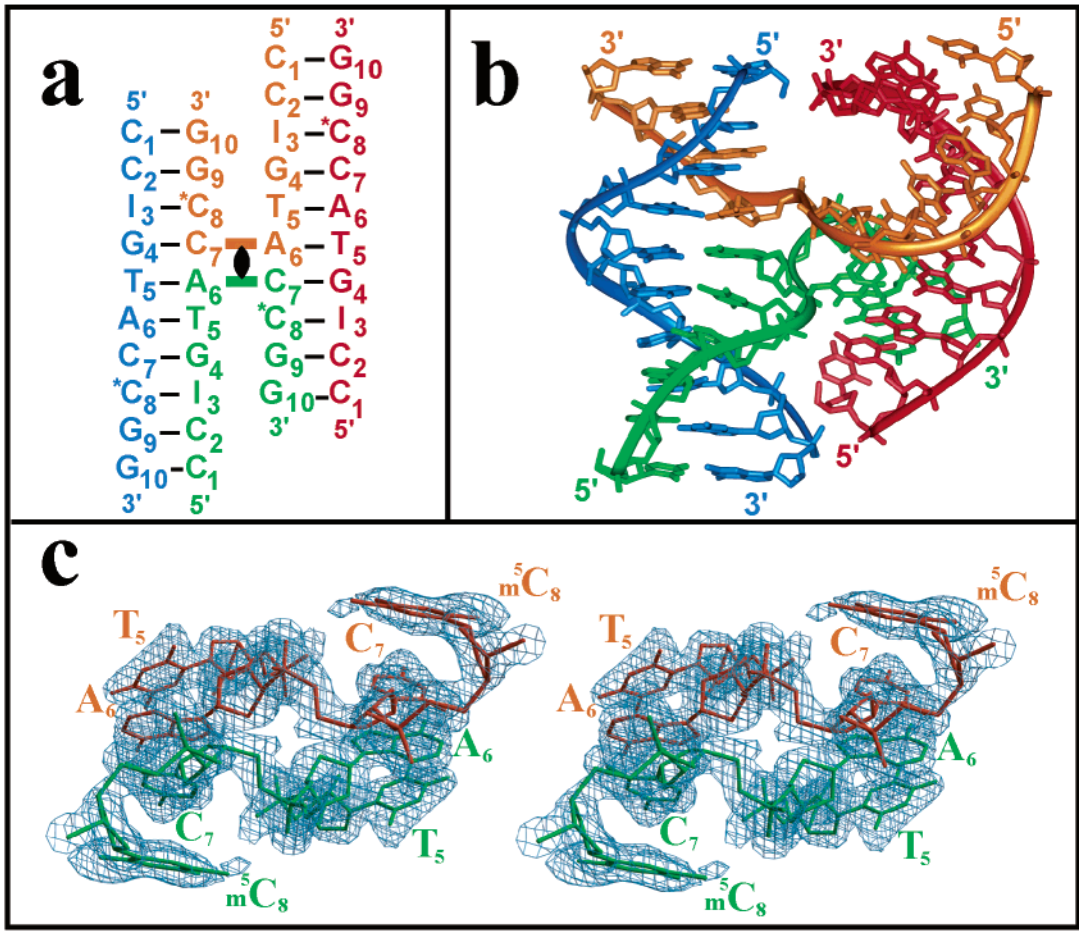

FIGURE 3: DNA Holliday junction crystal structure of d(CCIGTACm^{5}CGG). (a) Nomenclature used for the d(CCIGTACm^{5}CGG) junction with the full four-stranded complex generated by the application of a crystallographic 2-fold symmetry axis to the two unique strands (blue and orange). An asterisk adjacent to the eighth nucleotide in each decamer sequence denotes the presence of a 5-methylcytosine base. (b) Atomic structure of the d(CCIGTACm^{5}CGG) DNA Holliday junction. Nucleotides are rendered as sticks with the phosphodeoxyribose backbone rendered as a solid ribbon with the 5′ and 3′ ends labeled accordingly (this panel rendered with InsightII from MSI/Biosym, Inc.). (c) The final $2F_o - F_c$ electron density (contoured at 1σ) depicting the junction crossover region with continuous density between nucleotides A_6 and C_7 of the junction crossover strands. Nucleotides T_5, A_6, C_7, and m^5C_8 are rendered as sticks. The coloring scheme and strand designations in all panels are the same [this panel created with Bobscript (*53*) and rendered in Raster3D (*54*)].

this study demonstrates that specific atomic interactions which have been identified at the major groove surface of the trinucleotide core region of DNA Holliday junctions are specific for G·C base pairs in the major groove and do not accommodate A·T base pair substituents. Furthermore, the inosine junction structure provides an opportunity for direct comparison with the parent d(CCGGTACm^{5}CGG) junction structure (ACm^{5}C junction) in determining whether the minor groove 2-amino group in the R_3-Y_8 base step helps to define the geometry of the junction conformation.

Structure of d(CCIGTACm^{5}CGG) as a Holliday Junction. The single-crystal structure of the d(CCIGTACm^{5}CGG) sequence (iACm^{5}C junction) is a DNA Holliday junction in the right-handed antiparallel stacked-X conformation. The full four-stranded structure consists of two unique strands, one crossover and one noncrossover, related by a crystallographic 2-fold symmetry axis with the crossover occurring between nucleotides A_6 and C_7 of each set of pseudocontinuous B-DNA duplexes. These duplexes are formed by the stacking of a shorter four-base pair arm (nucleotides C_1-G_4 of an outside noncrossover strand with C_7-G_{10} from a crossover strand) onto a longer six-base pair arm (nucleotides T_5-G_{10} of an outside strand stacked on nucleotides C_1-A_6 of a crossover strand) (Figure 3).

The overall conformation of this junction, indeed of any crystal structure of four-stranded junctions, can be described by the geometric relationships between the set of stacked B-DNA arms and the center of the junction. We have defined these relationships and how they can be accurately measured very explicitly elsewhere (*18*, *39*), and will briefly describe them here. The most easily recognized of these relationships is the interduplex angle (IDA), which is the angle that relates the ends of the stacked arms to the center of the junction crossover. This is the angle that was estimated to be ~60° in solution and by AFM for synthetic junctions (*7*, *8*, *40*−*42*) that are fixed by sequence complementarity of four unique strands. The IDA when measured in this way, however, is a length-dependent parameter; therefore, we have defined the parameter J_{twist} as a measure of the angle formed by the helical axes projected onto the resolving plane of the junction. This is length-independent and, thus, is a more general descriptor for the angle relating the stacked arms of this structure. In addition, the stacked B-DNA arms can translate along and rotate about their respective helix axes.

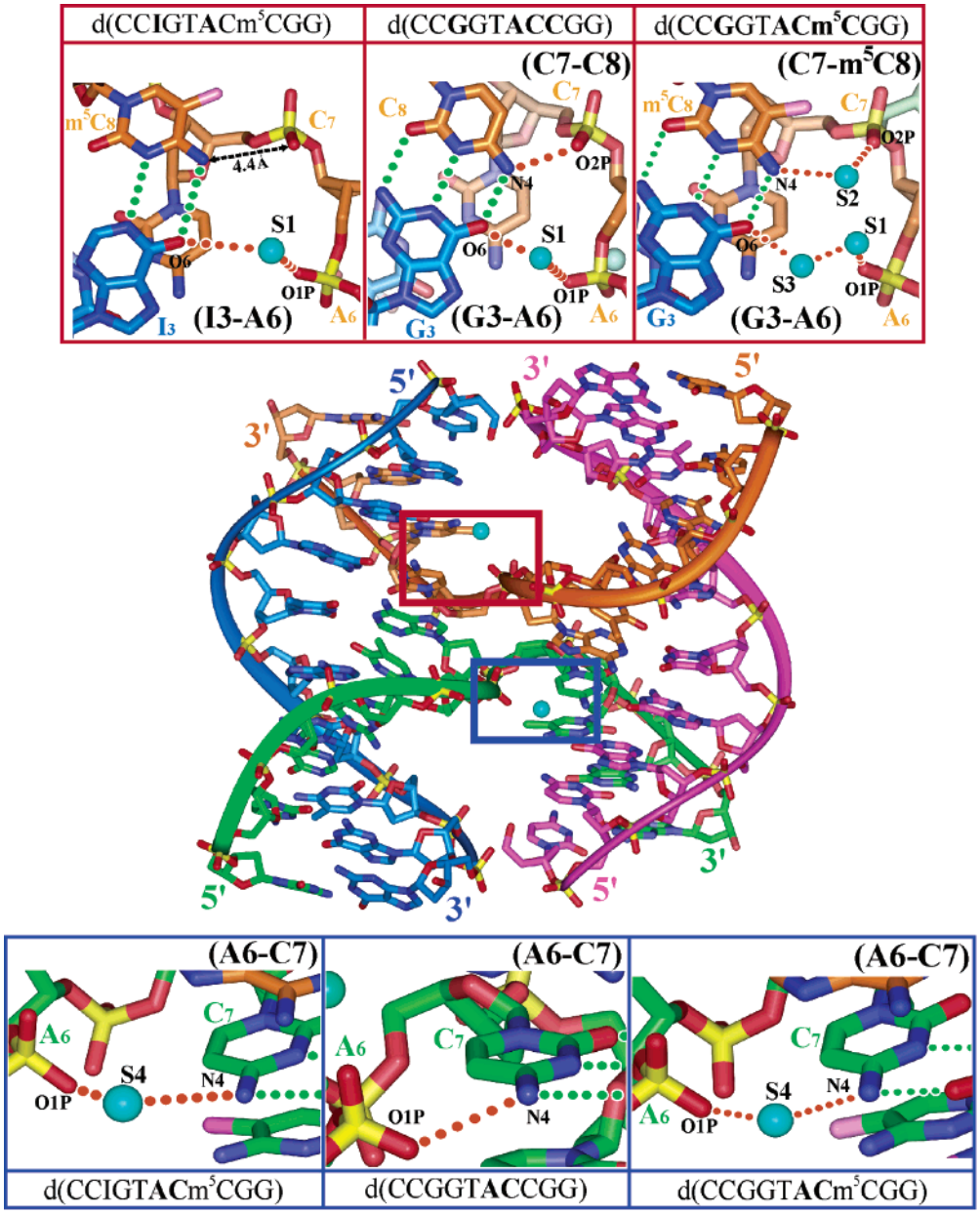

FIGURE 4: Stabilizing interactions within the stacked-X core region. The structure of the parent ACm^{5}C junction is shown with the location of the $R_6C_7Y_8$ trinucleotide core region hydrogen bonding interactions denoted with boxes. The area within these boxes is enlarged, as indicated by the corresponding box colors (red and blue), providing more detailed information about each stabilizing interaction. For comparison, the core region interactions are also shown for the unperturbed junction structure of the sequence d(CCGGTACCGG) (*15*). Within these inset boxes, Watson−Crick hydrogen bonding interactions are represented with green circles while core region atomic interactions with orange circles. The C_7-Y_8 and R_3-N_6 interactions are shown at the top, while the A_6-C_7 interaction is shown in the bottom box. DNA atoms are rendered as sticks and colored by strand with the respective 3′ and 5′ termini noted. No direct or solvent-mediated interaction is observed between the C_7 O2P and m^{5}C$_8$ N4 atoms (the distance between these atoms is 4.4 Å as indicated by the black arrow) within the iACm^{5}C-J structure.

These are reflected in the parameters J_{slide} and J_{roll}, respectively. The actual IDA for any crystal structure is thus a function of J_{twist}, J_{slide}, J_{roll}, and the length of each arm.

The structure of the iACm^{5}C junction is nearly identical to that of the parent ACm^{5}C junction in terms of its global geometry and detailed interactions. The global conformation of the iACm^{5}C junction structure (J_{slide} = 2.23 Å, J_{twist} = 42.5°, J_{roll} = 143.6°, and IDA = 61.4°) is nearly identical to that of the parent ACm^{5}C junction (J_{slide} = 2.25 Å, J_{twist} = 44.3°, J_{roll} = 145.9°, and IDA = 60.0°) in terms of these geometric parameters and as measured by the rmsd between like atoms (0.510 Å). The detailed interactions within the iACm^{5}C junction are also very similar to those of the parent structure, with minimal deviations. We have previously observed (*15*, *16*, *18*) that the global junction conformation is dependent on a set of key atomic interactions at the trinucleotide core region (Figure 4). These interactions include (i) a direct hydrogen bond between the exocyclic amine of C_8 and a phosphate oxygen on the C_7 backbone phosphate (C_7-Y_8 interaction), (ii) a solvent-mediated interaction between the outside R_3 (R is either an adenine or guanine nucleotide) keto oxygen and a phosphate oxygen of N_6 (R_3-N_6 interaction), and (iii) a direct hydrogen bond between the O1P phosphate oxygen of N_6 and the exocyclic

amine of C_7 (N_6-C_7 interaction). Consistent with this observation, we see here that the solvent-mediated interaction between the I_3 and A_6 nucleotides (R_3-N_6 interaction) is indeed present and mediated by a solvent molecule similar to that seen in the original d(CCGGTACCGG) junction (*15*). The N_6-C_7 interaction is also present and mediated by a solvent molecule similar to the parent ACm^{5}C junction structure (*18*). It was surprising that no direct or solvent-mediated interaction was observed between the N4 exocyclic amine of C_8 and the O1P phosphate oxygen of C_7 (C_7-Y_8 interaction) in this inosine-containing structure. This C_7-Y_8 interaction had been observed as a direct or solvent-mediated set of hydrogen bonding interactions in all but one of the previous DNA Holliday junction structures, suggesting that it is significant. In the case of the one previous exception and the current structure, the distance between O2P of C_7 and N4 of C_8 is similar to that when solvent-mediated interactions have been observed, suggesting that solvent is present, but was not resolved in the crystal structures.

Inosine has been shown to affect structural details of the DNA duplex, including groove widths, solvent interactions, and flexibility. In this case, we observe similar effects on the B-DNA arms of the iACm^{5}C junction. The width of the minor groove (as measured by the distance from the I_3 to G_9 backbone phosphorus atoms) adjacent to the I_3·m$^5C_8$ base pair is narrowed by 0.6 Å relative to that of the parent ACm^{5}C junction. This had previously been attributed to the loss of the minor groove 2-amino group (*35*, *36*, *43*, *44*). This narrower groove disrupts the solvent structure within the groove. Most notably, the hexaaquo-calcium(II) ion that sits in the minor groove at nucleotide positions G_3 and C_8 in the ACm^{5}C junction is no longer present in the current structure (Figure 5), yet the global conformation of the iACm^{5}C junction is nearly identical to that of the ACm^{5}C junction. Thus, we can conclude that the presence of the minor groove calcium ion in the ACm^{5}C junction does not contribute significantly to the perturbed conformation. The absence of this calcium ion was rather surprising given the 20-fold higher $CaCl_2$ concentration in the crystallization solutions of the iACm^{5}C junction as compared to that for the ACm^{5}C junction. In fact, no cations were identified in the structure of the iACm^{5}C junction, although the solvent is located in the proximity of the position where the calcium ion has been identified in previous junction structures (Figure 5). Any attempt to model this solvent as a calcium ion, even with reduced occupancies, resulted in a significant increase in R_{free}. Additionally, there is no ordered solvent around this location in the electron density maps that indicate anything other than water molecules in the minor groove.

The loss of the minor groove 2-amino group not only disrupts the solvent interactions but also increases the propeller twist of the I_3·m$^5C_8$ base pair and the G_4·C_7 base pair 3′ to the inosine base (Table 2). These perturbations are thought to increase the duplex flexibility in the region missing a minor groove 2-amino group (*20*, *36*). Greater flexibility is often manifested by an increase in propeller twist (*45*) and alteration of the backbone as observed by the presence of the BII backbone conformation (*43*, *46*). It is interesting to note that both inosine residues within the iACm^{5}C junction adopt the unusual BII conformation, which is consistent with these previous studies. Comparison of the inosine junction with the parent ACm^{5}C junction shows that

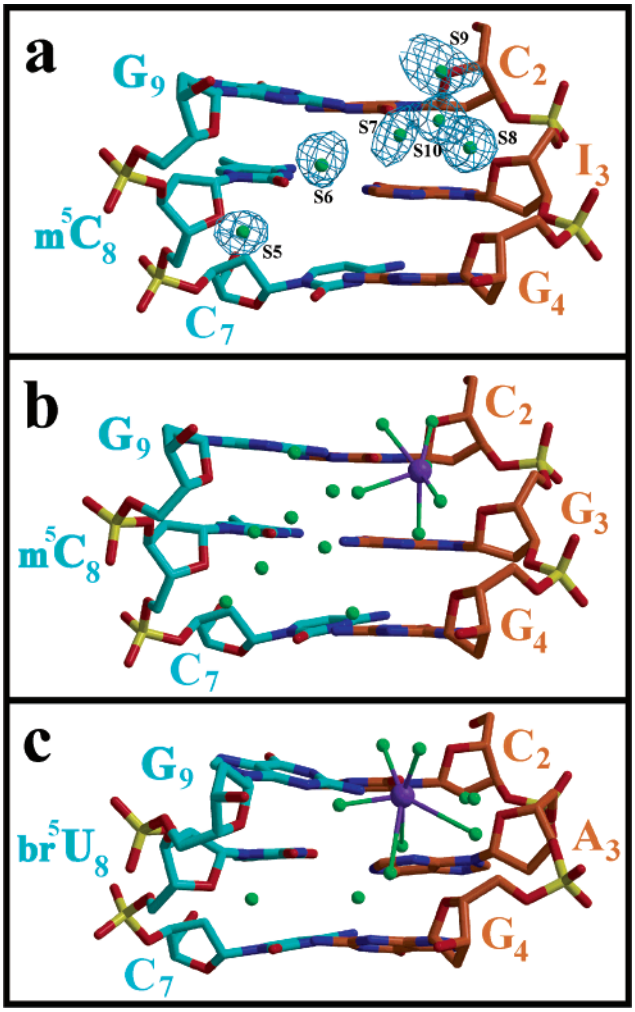

FIGURE 5: Minor groove solvent interactions adjacent to the R_3·Y_8 base step in DNA Holliday junctions. (a) Minor groove of the d(CCIGTACm^{5}CGG) structure between the C_2·G_9 and G_4·C_7 base pairs. The final $2F_o - F_c$ electron density (contoured at 1σ) is shown in blue for minor groove solvent molecules assigned within this region. Solvent molecules are labeled with the following distances between solvent waters S7−S9 and S10: S7−S10 distance = 2.9 Å, S8−S10 distance = 4.2 Å, and S9−S10 distance = 2.6 Å. (b) Minor groove of the d(CCGGTACm^{5}CGG) Holliday junction structure. (c) Minor groove of the d(CCAGTACbr^{5}UGG) Holliday junction structure. The view for all panels is looking into the minor groove with solvent water rendered as green spheres and calcium ions rendered as purple spheres. Interactions between calcium ions and solvent water are denoted with solid lines colored green and purple. All nucleotides are rendered as sticks and colored according to atom type [this figure created with Bobscript (*53*) and rendered in Raster3D (*54*)].

both guanine residues in the corresponding positions of the ACm^{5}C junction also adopt this unusual backbone conformation. Upon closer inspection of the junction structures, it is apparent that the unusual backbone conformation in this location of the structures results from crystal packing interactions and not a loss of the 2-amino group in the minor groove. Additionally, a BII conformation observed in the inosine structure for G_{19}, yet not observed in the ACm^{5}C junction, is also caused by crystal packing interactions (O1P of G_{19} is 3.3 Å from a symmetry-related O3′ of G_{20}). Thus, there is no clear indication from the iACm^{5}C junction structure that loss of the minor groove 2-amino groove results in greater flexibility of the B-DNA arms. Comparison of

Table 2: Comparison of Conformational Parameters for DNA Holliday Junction Structures of the d(CCGGTACm^{5}CGG) (ACm^{5}C-J), d(CCIGTACm^{5}CGG) (iACm^{5}C-J), and d(CCAGTACBr^{5}UGG) (ACBr^{5}U-J) Sequences and B-DNA Structures of d(CCAGTACTGG) in the Monoclinic (ACT-B-*C*2) and Hexagonal (ACT-B-*P*6$_1$22) Crystal Forms, d(CCDGTACTGG) (dACT-B), and d(CCGGCGCCGG) (GCC-B)

		ACm^{5}C-J	iACm^{5}C-J	ACBr^{5}U-J	ACT-B		dACT-B	GCC-B
space group (ref)[a]		*C*2 (*18*)	*C*2 (this paper)	*C*2 (*16*)	*C*2 (*47*)	*P*6$_1$22 (*15*)	*P*6$_1$22 (this paper)	*C*2 (*15*)
minor groove width (Å)[b]	C_2·G_9/Pu_3·Py_8	17.14	16.80	17.04	16.66	17.06	17.41	17.37
	Pu_3·Py_8/G_4·C_7	17.62	17.00	17.40	18.00	18.20	18.10	17.80
ζ dihedral angle (deg)	Pu_3	171.1 (BII)	134.0 (BII)	−105.4 (BI)	−86.2 (BI)	−81.5 (BI)	−100.4 (BI)	152.4 (BII)
	Pu_{13}	167.0 (BII)	170.2 (BII)	−94.6 (BI)	N/A	N/A	N/A	128.5 (BII)
	Py_8	167.9 (BII)	−173.4 (BI)	152.9 (BII)	164.9 (BII)	−158.4 (BI)	−102.6 (BI)	−127.9
	G_{19}	−173.0 (BI)	179.3 (BII)	−145.7 (BI)	N/A	N/A	N/A	−114.1
helical								
X-displacement (Å)	C_2·G_9	2.11	1.61	0.98	1.01	0.72	−1.19	0.02
	Pu_3·Py_8	2.11	1.69	0.70	0.83	−0.30	−1.13	0.51
tip (deg)	C_2·G_9	−0.56	−1.19	2.46	2.88	−5.17	−6.95	−0.84
	Pu_3·Py_8	−6.37	4.30	−23.46	−18.02	−16.36	−11.57	−0.68
base pair								
propeller twist (deg)	C_2·G_9	−7.6	−8.7	−22.8	−30.4	−22.3	−7.1	−14.4
	Pu_3·Py_8	−2.8	−8.7	−10.0	−20.7	−23.1	−18.0	3.8
	G_4·C_7	−15. 8	−40.0	−16.5	−8.6	−20.5	−16.5	−11.8
stagger (Å)	C_2·G_9	0.28	0.70	0.59	0.27	−0.10	0.41	−0.57
	Pu_3·Py_8	0.15	−0.46	0.35	0.24	0.14	−0.63	−0.15
	G_4·C_7	−0.05	−1.39	−0.22	0.34	−0.01	−0.02	0.17
buckle (deg)	C_2·G_9	−0.8	−7.8	−0.5	−2.3	3.7	−1.3	3.1
	Pu_3·Py_8	4.6	7.3	−2.9	−3.1	−4.2	4.3	0.0
	G_4·C_7	0.6	−6.1	7.5	14.9	11.6	−10.2	4.6
dimer step								
helical twist (deg)	C_2·G_9/Pu_3·Py_8	37.0	25.0	43.4	50.5	49.0	39.0	36.3
	Pu_3·Py_8/G_4·C_7	36.7	42.4	32.6	23.2	26.9	37.7	35.8
roll (deg)	C_2·G_9/Pu_3·Py_9	−5.8	5.5	−25.9	−20.9	−11.2	−4.6	0.2
	Pu_3·Py_8/G_4·C_8	2.4	−12.4	7.4	17.9	5.5	3. 6	−2.9
slide (Å)	C_2·G_9/Pu_3·Py_{10}	0.27	0.51	0.91	1.05	0.98	0.45	0.35
	Pu_3·Py_8/G_4·C_9	−0.05	0.35	−0.57	0.19	0.08	−0.42	0.08
shift (Å)	C_2·G_9/Pu_3·Py_{11}	0.00	0.08	−0.28	−0.18	−1.01	0.05	0.49
	Pu_3·Py_8/G_4·C_{10}	−1.03	−0.80	−0.66	0.35	0.26	0.81	−0.62
rise (Å)	C_2·G_9/Pu_3·Py_{12}	3.47	3.10	3.54	3.56	3.57	3.35	3.59
	Pu_3·Py_8/G_4·C_{11}	3.50	3.70	3.11	3.03	3.26	3.85	3.42
tilt (deg)	C_2·G_9/Pu_3·Py_{13}	−0.99	8.25	−5.87	−6.88	−12.69	3.85	−2.51
	Pu_3·Py_8/G_4·C_{12}	−8.03	−0.25	−12.17	−8.15	−11.49	−10.54	−3.28

[a] References are provided for published structures. [b] Minor groove interstrand width as measured by the P−P distance across adjacent dinucleotide steps (*52*). The sums of the van der Waals radii (5.8 Å) for the two phosphate groups have not been subtracted from the reported values.

crystallographic *B*-factors between these two junctions shows the same general patterns with no apparent increase in mobility or disorder of the inosine bases (average *B*-factor for DNA atoms in the iACm^{5}C structure of 11.1 Å^2 vs 13.9 Å^2 in the ACm^{5}C junction).

B-DNA Structure of d(CCDGTACTGG). The d(CCDGTACTGG) sequence (dACT structure) crystallized as resolved B-DNA duplexes with one unique strand in the asu, and the second strand of the duplex was generated by a crystallographic 2-fold symmetry axis (Figure 6). Having a single DNA strand in the asu precludes this structure from being a DNA Holliday junction, since a junction requires a minimum of two strands in the asu (one crossover and one noncrossover strand). This B-DNA duplex contains a D·T base pair which has base substituents in the major groove that are identical to an A·T base pair and substituents in the minor groove that are identical to a G·C base pair (Figure 2). The crystallization of this D·T base pair-containing sequence as resolved B-DNA duplexes demonstrates that the 2-amino group at the purine R_3 base is not sufficient for defining a junction in this lattice system and, therefore, further supports the model in which it is the major groove interactions at the trinucleotide core that are responsible for stabilization of the four-stranded conformation in crystals.

The B-DNA structure of dACT is very similar but not identical to those of the parent sequence d(CCAGTACTGG) in the hexagonal (rmsd = 1.17 Å for like non-hydrogen atoms, ACT-*P*6$_1$22) (*16*) and monoclinic (rmsd = 2.01 Å for like non-hydrogen atoms, ACT-*C*2) space groups (*47*). This observation that the ACT B-DNA structure can be crystallized in essentially the same monoclinic *C*2 space group as nearly all of the crystals of junctions suggests that the lattice system does not preclude and, indeed, can accommodate either DNA conformation. Thus, by extension, the effects on the structure of the B-DNA duplex from introduction of a 2-amino group into the minor groove appear to be independent of crystal type. The dACT structure reported here and ACT-*P*6$_1$22 are in the same crystal lattice (*P*6$_1$22) with very similar crystal packing interactions. We do, however, observe crystal packing interactions that cause minor perturbations to the local base geometry (such as the close approach of the C_7 base with a symmetry-related phosphate group of A_6).

We should note that there are noticeable deviations from ideal geometry in the dACT structure as noted by the high rmsd values for the bond lengths and angles in this structure (Table 1) for which crystal packing interactions cannot entirely account [the analogous ACT-*P*6$_1$22 exhibits overall rmsd values for bond lengths and angles that are very close to ideal (*16*)]. Divalent cations have previously been shown to cause significant perturbations to DNA structures (*38*). Thus, it may be the presence of two hexaaquo-calcium(II)

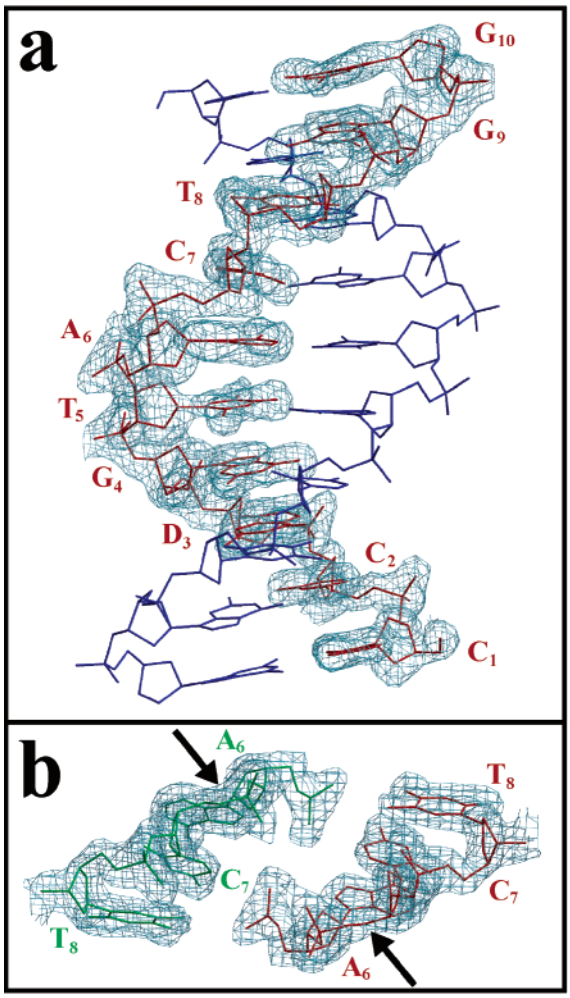

FIGURE 6: Structure of d(CCDGTACTGG). (a) Structure of d(CCDGTACTGG) as a B-DNA double helix in the $P6_122$ crystal form. The final $2F_o - F_c$ electron density (contoured at 1σ) depicting the unique asymmetric unit strand (rendered as red sticks) which sits adjacent to a crystallographic symmetry axis. (b) The final $2F_o - F_c$ electron density (contoured at 1σ) depicting the closest approach between two duplexes. Arrows denote the points at which the phosphoribose backbone would deviate if this sequence were to form a junction. Since the structure of d(CCDGTACTGG) has only one strand in the asu, we can conclude with certainty that this sequence does not form a DNA Holliday junction, as a minimum of two unique strands are required for junction structures [this figure created with Bobscript (*53*) and rendered in Raster3D (*54*)].

ions interacting with the C_7 and A_6 nucleobases that are responsible for significant distortions to the bases from their ideal geometries.

Introduction of a minor groove 2-amino group has been shown to increase the minor groove width, increase helical twist, and alter the general base characteristics such as shift, slide, rise, tilt, roll, and propeller twist of nucleotides within B-DNA duplexes (*35*, *36*, *43*, *44*). Indeed, we see a significant increase in the helical twist for the D·T base pair by ~10.8° when compared to the corresponding step in the ACT structures, and 2° greater compared to the corresponding step in the B-DNA structure of d(CCGGCGCCGG) (GCC-B) (*48*). This increase in helical twist does not extend to the overall twist of the duplex. The average helical twist for the dACT duplex is 34.5° (SD = 5.1°), which is similar to the value of 35.3° for ACT-$P6_122$ [SD = 8.8° (*16*)] structure and 36.3° for the ACT-*C*2 [SD = 10.3° (*47*)] structure. Thus, the dACT B-DNA structure is not overwound overall, even though the individual D·T base pairs display greater helical twist. Furthermore, there is a 0.75 Å increase in the minor groove width around the D·T base pair when compared to that in the ACT-*C*2 structure (*47*) and a 0.35 Å increase when compared to that of the ACT-$P6_122$ structure. This widening is expected from the addition of the 2-amino group in this location.

The presence of a 2-amino group in the minor groove is also known to disrupt the spine of hydration which is commonly observed in the minor groove of B-DNA duplexes (*49*). Indeed, we see a disruption of solvent in the distal regions of the minor groove adjacent to the 2-amino group of the 2,6-diaminopurine relative to the parent d(CCAGTACTGG) structures. Thus, we can see that the introduction of the 2,6-diaminopurine base into the d(CCDGTACTGG) B-DNA structure results in a D·T base pair which is more G·C-like than A·T-like in terms of general characteristics of the minor groove (Table 2) yet still forms resolved B-DNA duplexes and not a four-way junction.

CONCLUSIONS

We determined the single-crystal structures of DNA sequences d(CCIGTACm^{5}CGG) and d(CCDGTACTGG) to elucidate the effect of major and minor groove substituents on the formation of four-stranded Holliday junctions. The two sequences differ from their parent sequences, d(CCGGTACm^{5}CGG) and d(CCAGTACTGG), respectively, by the presence of an I·m^{5}C or D·T base pair in the third step, thus either eliminating or adding an amino substituent in the purine 2-position of the G_3·C_8 base pair or the A_3·T_8 base pair of the respective structures. This renders the I·m^{5}C base pairs G·C-like in the major groove and A·T-like in the minor groove, while D·T base pairs are A·T-like in the major groove and G·C-like in the minor groove (Figure 2). The sequence d(CCIGTACm^{5}CGG) was seen to crystallize as a DNA Holliday junction in a right-handed antiparallel stacked-X configuration just like its parent sequence, while the d(CCDGTACTGG) sequence formed resolved B-DNA duplexes, again like its parent sequence. Thus, we can conclude that the minor groove substituents at the $N_6C_7Y_8$ trinucleotide core motif do not play a significant role in the formation of four-stranded junctions.

There are, however, effects from the 2-amino substituent on the conformation and solvent structure of the duplex arms and, indirectly, on the major groove interactions that help us to focus on those structural features that are important and not important in defining the conformation of the Holliday junction in this crystal system. It is now clear that the width of the helix in and around the crossover point does not affect the formation or geometry of the junction. Narrowing the minor groove by removing the 2-amino group does not interfere with the junction, while widening it by the introduction of this group does not induce its formation. The associated solvent rearrangements, including displacement of cations resulting from the narrowing of the minor groove, have little effect on the geometry of the junction. The overwinding or underwinding of the helix and buckling or propeller twist of the base pairs also have little effect. This study, therefore, reinforces our contention that the conformations of the helical arms are determined primarily

by the sequence-dependent features of the arms and are only minimally perturbed by the junction, and that the junction can accommodate a number of conformational variations in these arms. The compensatory over- and underwinding of the helix (as seen in the increased helical twist around the inosine bases, but associated underwinding of adjacent base pairs to give an average helical twist that is similar to that of the parent junction) suggest that the long-range interactions between arms, as previously proposed (*50*), may remain an important component of the junction.

Perhaps the most significant result from this study is that we can now distinguish two specific interactions at the major groove surface that are the primary determinants of the junction geometry. Specifically, the hydrogen bonds from the Y_8 amino nitrogen to the crossover phosphate oxygen at C_7 and the amino nitrogen of C_7 to the A_6 phosphate oxygen of the opposing duplex arm, whether they are direct or solvent-mediated, are the two defining interactions. The hydrogen bond from R_3 to the A_6 phosphate oxygen of the adjacent duplex can be mediated by one or two intervening solvent molecules without significantly affecting the conformation. Additionally, the monovalent cation at the center of the original d(CCGGTACCGG) junction structure was previously shown not to play a significant role in defining the junction conformation (*16*). Thus, the conformation and structural variability of the antiparallel stacked-X Holliday junction appear to hinge on only these two specific interactions, and it is the perturbation of these interactions by sequence, base substituents, or drugs and ions that defines the gross geometric features of this recombination intermediate.

ACKNOWLEDGMENT

We thank Ganapathy Sarma for helpful discussions during preparation of the manuscript.

REFERENCES

1. Holliday, R. (1964) A mechanism for gene conversion in fungi, *Genet. Res. 5*, 282−304.
2. Liu, Y., Masson, J. Y., Shah, R., O'Regan, P., and West, S. C. (2004) RAD51C is required for Holliday junction processing in mammalian cells, *Science 303*, 243−246.
3. Wu, L., and Hickson, I. D. (2003) The Bloom's syndrome helicase suppresses crossing over during homologous recombination, *Nature 426*, 870−874.
4. Rafferty, J. B., Bolt, E. L., Muranova, T. A., Sedelnikova, S. E., Leonard, P., Pasquo, A., Baker, P. J., Rice, D. W., Sharples, G. J., and Lloyd, R. G. (2003) The structure of *Escherichia coli* RusA endonuclease reveals a new Holliday junction DNA binding fold, *Structure 11*, 1557−1567.
5. Dickman, M. J., Ingleston, S. M., Sedelnikova, S. E., Rafferty, J. B., Lloyd, R. G., Grasby, J. A., and Hornby, D. P. (2002) The RuvABC resolvasome, *Eur. J. Biochem. 269*, 5492−5501.
6. Subramaniam, S., Tewari, A. K., Nunes-Duby, S. E., and Foster, M. P. (2003) Dynamics and DNA substrate recognition by the catalytic domain of lambda integrase, *J. Mol. Biol. 329*, 423−439.
7. Cooper, J. P., and Hagerman, P. J. (1989) Geometry of a branched DNA structure in solution, *Proc. Natl. Acad. Sci. U.S.A. 86*, 7336−7340.
8. Duckett, D. R., Murchie, A. I., Diekmann, S., von Kitzing, E., Kemper, B., and Lilley, D. M. (1988) The structure of the Holliday junction, and its resolution, *Cell 55*, 79−89.
9. von Kitzing, E., Lilley, D. M., and Diekmann, S. (1990) The stereochemistry of a four-way DNA junction: a theoretical study, *Nucleic Acids Res. 18*, 2671−2683.
10. McKinney, S. A., Declais, A. C., Lilley, D. M., and Ha, T. (2003) Structural dynamics of individual Holliday junctions, *Nat. Struct. Biol. 10*, 93−97.
11. Grainger, R. J., Murchie, A. I., and Lilley, D. M. (1998) Exchange between stacking conformers in a four-way DNA junction, *Biochemistry 37*, 23−32.
12. Miick, S. M., Fee, R. S., Millar, D. P., and Chazin, W. J. (1997) Crossover isomer bias is the primary sequence-dependent property of immobilized Holliday junctions, *Proc. Natl. Acad. Sci. U.S.A. 94*, 9080−9084.
13. Hays, F. A., Watson, J., and Ho, P. S. (2003) Caution! DNA crossing: crystal structures of Holliday junctions, *J. Biol. Chem. 278*, 49663−49666.
14. Ho, P. S., and Eichman, B. F. (2001) The crystal structures of DNA Holliday junctions, *Curr. Opin. Struct. Biol. 11*, 302−308.
15. Eichman, B. F., Vargason, J. M., Mooers, B. H., and Ho, P. S. (2000) The Holliday junction in an inverted repeat DNA sequence: sequence effects on the structure of four-way junctions, *Proc. Natl. Acad. Sci. U.S.A. 97*, 3971−3976.
16. Hays, F. A., Vargason, J. M., and Ho, P. S. (2003) Effect of sequence on the conformation of DNA Holliday junctions, *Biochemistry 42*, 9586−9597.
17. Sha, R., Liu, F., and Seeman, N. C. (2002) Atomic force microscopic measurement of the interdomain angle in symmetric Holliday junctions, *Biochemistry 41*, 5950−5955.
18. Vargason, J. M., and Ho, P. S. (2002) The effect of cytosine methylation on the structure and geometry of the Holliday junction: the structure of d(CCGGTACm5CGG) at 1.5 Å resolution, *J. Biol. Chem. 277*, 21041−21049.
19. Lankas, F., Cheatham, T. E., III, Spackova, N., Hobza, P., Langowski, J., and Sponer, J. (2002) Critical effect of the N2 amino group on structure, dynamics, and elasticity of DNA polypurine tracts, *Biophys. J. 82*, 2592−2609.
20. Cubero, E., Guimil-Garcia, R., Luque, F. J., Eritja, R., and Orozco, M. (2001) The effect of amino groups on the stability of DNA duplexes and triplexes based on purines derived from inosine, *Nucleic Acids Res. 29*, 2522−2534.
21. Lavigne, M., and Buc, H. (1999) Compression of the DNA minor groove is responsible for termination of DNA synthesis by HIV-1 reverse transcriptase, *J. Mol. Biol. 285*, 977−995.
22. Teplukhin, A. V., Poltev, V. I., and Chuprina, V. P. (1991) Dependence of the hydration shell structure in the minor groove of the DNA double helix on the groove width as revealed by Monte Carlo simulation, *Biopolymers 31*, 1445−1453.
23. Woods, K. K., Lan, T., McLaughlin, L. W., and Williams, L. D. (2003) The role of minor groove functional groups in DNA hydration, *Nucleic Acids Res. 31*, 1536−1540.
24. Brennan, C. A., Van Cleve, M. D., and Gumport, R. I. (1986) The effects of base analogue substitutions on the methylation by the EcoRI modification methylase of octadeoxyribonucleotides containing modified EcoRI recognition sequences, *J. Biol. Chem. 261*, 7279−7286.
25. Brennan, C. A., Van Cleve, M. D., and Gumport, R. I. (1986) The effects of base analogue substitutions on the cleavage by the EcoRI restriction endonuclease of octadeoxyribonucleotides containing modified EcoRI recognition sequences, *J. Biol. Chem. 261*, 7270−7278.
26. Hamy, F., Asseline, U., Grasby, J., Iwai, S., Pritchard, C., Slim, G., Butler, P. J., Karn, J., and Gait, M. J. (1993) Hydrogen-bonding contacts in the major groove are required for human immunodeficiency virus type-1 tat protein recognition of TAR RNA, *J. Mol. Biol. 230*, 111−123.
27. Pastor, N., MacKerell, A. D., Jr., and Weinstein, H. (1999) TIT for TAT: the properties of inosine and adenosine in TATA box DNA, *J. Biomol. Struct. Dyn. 16*, 787−810.
28. Tuschl, T., Ng, M. M., Pieken, W., Benseler, F., and Eckstein, F. (1993) Importance of exocyclic base functional groups of central core guanosines for hammerhead ribozyme activity, *Biochemistry 32*, 11658−11668.
29. Kissinger, C. R., Gehlhaar, D. K., and Fogel, D. B. (1999) Rapid automated molecular replacement by evolutionary search, *Acta Crystallogr. D55* (Part 2), 484−491.
30. Brunger, A. T., Adams, P. D., Clore, G. M., DeLano, W. L., Gros, P., Grosse-Kunstleve, R. W., Jiang, J. S., Kuszewski, J., Nilges, M., Pannu, N. S., Read, R. J., Rice, L. M., Simonson, T., and Warren, G. L. (1998) Crystallography & NMR system: A new software suite for macromolecular structure determination, *Acta Crystallogr. D54* (Part 5), 905−921.

31. Otwinowski, Z., and Minor, W. (1997) Processing of X-ray Diffraction Data Collected in Oscillation Mode, *Methods Enzymol. 276*, 307−326.
32. McLachlan, A. D. (1982) Rapid Comparison of Protein Structures, *Acta Crystallogr. A38*, 871−873.
33. Lavery, R., and Sklenar, H. (1989) Defining the structure of irregular nucleic acids: conventions and principles, *J. Biomol. Struct. Dyn. 6*, 655−667.
34. Berman, H. M., Westbrook, J., Feng, Z., Gilliland, G., Bhat, T. N., Weissig, H., Shindyalov, I. N., and Bourne, P. E. (2000) The Protein Data Bank, *Nucleic Acids Res. 28*, 235−242.
35. Lan, T., and McLaughlin, L. W. (2001) Minor groove functional groups are critical for the B-form conformation of duplex DNA, *Biochemistry 40*, 968−976.
36. Sun, Z., Chen, D., Lan, T., and McLaughlin, L. W. (2002) Importance of minor groove functional groups for the stability of DNA duplexes, *Biopolymers 65*, 211−217.
37. Chiu, T. K., and Dickerson, R. E. (2000) 1 Å crystal structures of B-DNA reveal sequence-specific binding and groove-specific bending of DNA by magnesium and calcium, *J. Mol. Biol. 301*, 915−945.
38. Minasov, G., Tereshko, V., and Egli, M. (1999) Atomic-resolution crystal structures of B-DNA reveal specific influences of divalent metal ions on conformation and packing, *J. Mol. Biol. 291*, 83−99.
39. Watson, J., Hays, F. A., and Ho, P. S. (2004) Definitions and Analysis of DNA Holliday Junction Geometry, *Nucleic Acids Res. 32*, 1−11.
40. Cooper, J. P., and Hagerman, P. J. (1987) Gel electrophoretic analysis of the geometry of a DNA four-way junction, *J. Mol. Biol. 198*, 711−719.
41. Clegg, R. M., Murchie, A. I., Zechel, A., and Lilley, D. M. (1993) Observing the helical geometry of double-stranded DNA in solution by fluorescence resonance energy transfer, *Proc. Natl. Acad. Sci. U.S.A. 90*, 2994−2998.
42. Mao, C., Sun, W., and Seeman, N. C. (1999) Designed two-dimensional DNA Holliday junction arrays visualized by atomic force microscopy, *J. Am. Chem. Soc. 121*, 5437−5443.
43. Wellenzohn, B., Flader, W., Winger, R. H., Hallbrucker, A., Mayer, E., and Liedl, K. R. (2001) Exocyclic groups in the minor groove influence the backbone conformation of DNA, *Nucleic Acids Res. 29*, 5036−5043.
44. Xuan, J. C., and Weber, I. T. (1992) Crystal structure of a B-DNA dodecamer containing inosine, d(CGCIAATTCGCG), at 2.4 Å resolution and its comparison with other B-DNA dodecamers, *Nucleic Acids Res. 20*, 5457−5464.
45. el Hassan, M. A., and Calladine, C. R. (1996) Propeller-twisting of base-pairs and the conformational mobility of dinucleotide steps in DNA, *J. Mol. Biol. 259*, 95−103.
46. Hartmann, B., Piazzola, D., and Lavery, R. (1993) BI−BII transitions in B-DNA, *Nucleic Acids Res. 21*, 561−568.
47. Kielkopf, C. L., Ding, S., Kuhn, P., and Rees, D. C. (2000) Conformational flexibility of B-DNA at 0.74 Å resolution: $d(CCAGTACTGG)_2$, *J. Mol. Biol. 296*, 787−801.
48. Heinemann, U., Alings, C., and Bansal, M. (1992) Double helix conformation, groove dimensions and ligand binding potential of a G/C stretch in B-DNA, *EMBO J. 11*, 1931−1939.
49. Howard, F. B., and Miles, H. T. (1984) 2NH2A X T helices in the ribo- and deoxypolynucleotide series. Structural and energetic consequences of 2NH2A substitution, *Biochemistry 23*, 6723−6732.
50. Eichman, B. F., Ortiz-Lombardia, M., Aymami, J., Coll, M., and Ho, P. S. (2002) The inherent properties of DNA four-way junctions: comparing the crystal structures of Holliday junctions, *J. Mol. Biol. 320*, 1037−1051.
51. Brunger, A. T. (1992) Free *R* value: a novel statistical quantity for assessing the accuracy of crystal structures, *Nature 355*, 472−475.
52. El Hassan, M. A., and Calladine, C. R. (1998) Two distinct modes of protein-induced bending in DNA, *J. Mol. Biol. 282*, 331−343.
53. Esnouf, R. M. (1999) Further additions to MolScript version 1.4, including reading and contouring of electron-density maps, *Acta Crystallogr. D55* (Part 4), 938−940.
54. Merritt, E. A., and Bacon, D. J. (1997) Raster3D: Photorealistic Molecular Graphics, *Methods Enzymol. 277*, 505−524.

BI049461D